Downlink Femto-Macro ICIC with Location-Based Long-Term Power Setting

Julien Guillet, Loïc Brunel and Nicolas Gresset
Mitsubishi Electric R&D Centre Europe
1 Allée de Beaulieu, CS 10806, 35708 Rennes Cedex, France
Email: {j.guillet, l.brunel, n.gresset}@fr.merce.mee.com

***Abstract*—Inter-cell interference is a major issue in current wireless cellular systems, in particular with the development of femto-cells. Efficient macro-femto inter-cell interference coordination (ICIC) is crucial and should be performed with minimum communication between macro and femto base stations. We propose an ICIC approach, in which each femto base station informs a server about its position, obtains relevant information from mobile terminal measurements stored in a database maintained by the server and configures its transmission power according to this information. This power setting aims at maintaining a controlled impact of the femto base station on macro-cell performance, independent of the femto-cell location. In a 3GPP-LTE context, this approach exhibits a good femto-macro performance trade-off and is robust against power and positioning measurement errors.**

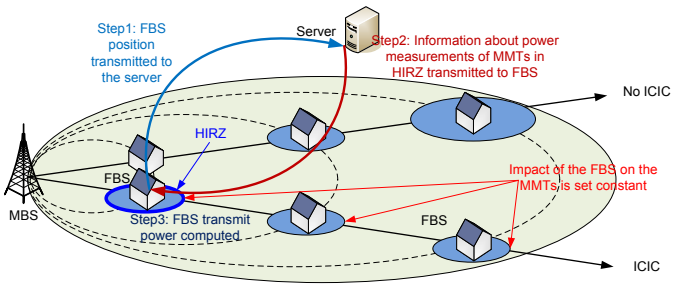

Fig. 1: ICIC providing macro-degradation equalization (single cell, no shadowing).

I. Introduction

In current mobile cellular networks, like 3GPP Long Term Evolution (LTE) networks, heterogeneous deployments mixing macro base stations (MBS) and home base stations or femto base stations (FBS) are foreseen as an effective way to ensure both mobility within a large geographical area and high data throughput at home [1][2]. As in homogeneous macro deployments, fairness between cell-center and cell-edge users [3] must be sought and inter-cell interference coordination (ICIC) [3][4] appears as a proper way to mitigate the interference impact. In heterogeneous co-channel deployments, FBSs may strongly interfere with MBSs and even create coverage holes in downlink (DL). In order to secure the operator MBS traffic, priority should be put on minimizing the interference created by FBSs on MBSs. However, the FBS throughput inside home should remain reasonably high. Furthermore, due to the high number of FBSs under the MBS coverage, macro-femto ICIC minimizing the MBS-FBS exchanges is desirable.

As depicted in Fig. 1, for the *No ICIC* case, the area where macro mobile terminals (MTs) are strongly interfered by the FBS varies, depending of the FBS position relative to MBSs.

In a DL macro-femto ICIC approach presented in [5], the FBS independently sets its long-term transmit power [6], [7] according to its knowledge of the additive white Gaussian noise (AWGN) level and the received power from neighboring MBSs. In [5], received powers are obtained through measurements performed by the FBS on MBS DL signals. From an operator point-of-view, it is desirable that the impact of a FBS on surrounding macro MTs (MMTs) is independent of its location in the MBS coverage. The power setting in [5] achieves this property, which we call here macro-degradation equalization. In addition to VoIP and data services, mobile cellular networks also propose positioning services [8]. Positioning is also implemented in most MTs through Global Navigation Satellite System (GNSS). In this paper, we investigate how the MT and FBS location information, together with the supply of an appropriate database, can benefit to the long-term ICIC power setting, by providing precise information on received powers at MMTs surrounding a given FBS.

After describing several key concepts of long-term power setting in Section II, we detail the proposed location-based FBS power setting in Section III. Finally, Section IV presents evaluation results for a 3GPP-LTE system and provides comparison with constant FBS transmit power and the FBS measurement based power setting approach of [5], including errors on measurements and propagation models.

II. Power setting principles

A. Inter-cell interference definition

We consider a planned macro-cellular system, serving MMTs, and FBSs with closed-subscriber group (CSG), e.g., private home base stations, serving femto mobile terminals (FMTs). We denote $P_{t,F}$ the transmit power of the most interfering FBS for a given MMT, G_F the path gain from this FBS to the MMT, P_M the received power at the MMT from the MBS serving the MMT, I the level of the interference received from other MBSs and FBSs plus AWGN at the MMT. The signal to interference plus noise ratio (SINR) for the MMT

is

$$SINR_M\left(P_{t,F}\right) = \frac{P_M}{I + P_{t,F}G_F} \quad . \tag{1}$$

Let us define a performance metric as an increasing function of the SINR. There is a trade-off between femto and macro performance driven by the FBS transmit power $P_{t,F}$. Long-term FBS power setting must ensure a controlled macro-femto performance trade-off for a high number of MMT and FMT SINR realizations.

B. Macro-degradation equalization

For the sake of macro-degradation equalization, we introduce a *high interference reference zone* (HIRZ) [5], as depicted in Fig. 1, which is a given area in which the level of MMT performance degradation is controlled. When the same HIRZ and the same definition and level of MMT performance degradation are considered for all FBSs, all FBSs are expected to have the same impact on the MMTs and macro-degradation equalization is achieved.

The HIRZ, denoted Z_{MMT}, is a ring encompassing the femto building. We define the macro performance degradation as a function $g(\cdot)$ being the ratio of the MMT performance metric with and without FBS transmission. As the path gain properties are not the same for all positions in Z_{MMT}, we consider the outage probability of the degradation function $g(\cdot)$. The FBS transmit power is set to $P_{t,F}^{sol}$ such that, in Z_{MMT}, the probability that $g\left(P_M, I, G_F P_{t,F}^{sol}\right)$ is lower than or equal to a threshold g_{th} equals P_{OUT}:

$$\Pr\left(g\left(P_M, I, G_F P_{t,F}^{sol}\right) \leq g_{th} | Z_{MMT}\right) = P_{OUT}. \tag{2}$$

It is equivalent to find the FBS transmit power $P_{t,F}^{sol}$ such that,

$$\Pr\left(P_{t,F}^{sol} \leq \frac{1}{G_F} g^{-1}\left(P_M, I, g_{th}\right) | Z_{MMT}\right) = P_{OUT}, \tag{3}$$

where $g^{-1}\left(P_M, I, g_{th}\right)/G_F$ is the appropriate power setting value for a given realization of P_M, G_F and I. Function $g^{-1}(\cdot)$ denotes the inverse function of $g(\cdot)$. Thus, the transmit power setting solution $P_{t,F}^{sol}$ can be expressed as a quantile function:

$$P_{t,F}^{sol} = Q_{\frac{1}{G_F} g^{-1}(P_M, I, g_{th}) | Z_{MMT}}\left(P_{OUT}\right), \tag{4}$$

where the quantile $Q_{u|Z_{MMT}}(P)$ denotes the input value of the cumulative distribution function (CDF) of function $u(\cdot)$ such as the CDF evaluated on the area Z_{MMT} equals P. Thus, the long-term power setting is defined by a choice of the function $g(\cdot)$, of the HIRZ Z_{MMT} and of the parameters g_{th} and P_{OUT}.

C. Power setting based on spectral efficiency degradation

We adopt a performance metric related to spectral efficiency S. The macro performance degradation is defined as

$$g\left(P_M, I, G_F P_{t,F}\right) = S\left(P_{t,F}\right)/S\left(0\right), \tag{5}$$

where

$$S\left(P_{t,F}\right) = a \log_2\left(1 + b \times SINR_M\left(P_{t,F}\right)\right). \tag{6}$$

Parameters a and b are chosen in order to accurately compute the obtained spectral efficiency from the large-scale SINR. For each MT, we compute the spectral efficiency, taking into account small-scale channel effects and scheduling, and the large-scale SINR. Finally, a and b are chosen in order to fit the obtained cloud of (large-scale SINR, spectral efficiency) couples. Using (1) in (5), we obtain

$$\frac{g^{-1}\left(P_M, I, g_{th}\right)}{G_F} = \frac{1}{G_F}\left(\frac{bP_M}{\left(1 + bP_M/I\right)^{g_{th}} - 1} - I\right). \tag{7}$$

The path gain G_F is modeled with a log-normal distribution and the exact distribution is obtained with FMT measurements or through a predefined path loss model. In the latter case, the variance is the shadowing variance and the mean is for instance obtained from a log-distance path loss model, using the mean radius of Z_{MMT} and assuming a given wall penetration loss A_w.

III. FBS TRANSMIT POWER COMPUTATION WITH POSITION INFORMATION

In the proposed location-based approach, the statistical model for P_M and I powers received from MBSs at MMTs in Z_{MMT} is based on the FBS position information and the use of a geo-referenced database. The geo-referenced database has been constructed in advance thanks to MMT reports to their serving MBS, containing received power from neighboring base stations and the MMT location. Upon installation or reinitialization, a FBS obtains its own location information, e.g., through GNSS, and transmits it to the server maintaining the database. Thanks to this information, the server can transfer appropriate information about MMTs located in Z_{MMT} to the FBS. This information allows accurate power setting at FBS.

This database approach, depicted in Fig. 1, induces different types of errors: FBS position error, MMT position errors, MMT power measurement errors and quantization errors. The FBS position error may be lower than the MMT position error since the FBS location remains unchanged for a long duration.

The information transferred by the server to the FBS may be obtained in at least two ways from measurements performed by MMTs in Z_{MMT}. It may be, in increasing order of accuracy,

- the mean $\overline{g^{inv}}|_{dB}$ and variance $\sigma^2_{g^{inv}|_{dB}}$ of the inverse degradation function $g^{-1}\left(\hat{P}_{M,i}, \hat{I}_i, g_{th}\right)|_{dB}$ over all samples i in Z_{MMT},
- or directly the samples of the inverse degradation function $g^{-1}\left(\hat{P}_{M,i}, \hat{I}_i, g_{th}\right)|_{dB}$,

where $\hat{P}_{M,i}$ and $\hat{I}_i$ are the database sample i for P_M and I, respectively, and $x|_{dB}$ is the expression of x in dB.

In the first approach, considering a log-normal distribution for $g^{-1}\left(P_M, I, g_{th}\right)$ and G_F and using (4), the quantile of a normal distribution has to be evaluated in order to get $P_{t,F}^{sol}$ in dB:

$$\begin{aligned} P_{t,F}^{sol}|_{dB} &= Q_{-G_F|_{dB} + g^{-1}(P_M, I, g_{th})|_{dB} | Z_{MMT}}\left(P_{OUT}\right) \\ &= -\overline{G}_F|_{dB} + \overline{g}^{inv}|_{dB} + \sigma|_{dB} Q_{\mathcal{N}}\left(P_{OUT}\right), \end{aligned} \tag{8}$$

where $Q_{\mathcal{N}}$ is the quantile function of the standard normal distribution. Assuming independence between the FBS-MMT path gain and the received power from MBS we obtain,

$$\sigma|_{dB} = \sqrt{\sigma^2_{G_F|_{dB}} + \sigma^2_{g^{inv}|_{dB}}}, \tag{9}$$

where $\overline{G}_F|_{dB}$ and $\sigma^2_{G_F|_{dB}}$ are the mean and variance of $G_F|_{dB}$ in area Z_{MMT}, respectively. In the second approach, still considering a log-normal distribution for G_F, independent of $\hat{P}_{M,i}$ and $\hat{I}_i$, (4) results in the computation of the quantile of a Gaussian mixture. Indeed, the distribution is the mixture of Gaussian distributions, the mean and variance of distribution i being $g^{-1}\left(\hat{P}_{M,i}, \hat{I}_i, g_{th}\right)|_{dB} + \overline{G}_F|_{dB}$ and $\sigma^2_{G_F|_{dB}}$, respectively. With $\sigma^2_{G_F|_{dB}}$ being large compared to the variance on database samples $g^{-1}\left(\hat{P}_{M,i}, \hat{I}_i, g_{th}\right)$, the first approach is a good approximation of the second one. This condition is satisfied in scenarios of interest and, in the sequel of this paper, we use the first approach. Therefore, with (8) and (9), the solution for femto transmit power setting is in log scale,

$$\begin{aligned} P^{sol}_{t,F}|_{dB} &= -\overline{G}_F|_{dB} + \overline{g}^{inv}|_{dB} \\ &\quad + \sqrt{\sigma^2_{G_F|_{dB}} + \sigma^2_{g^{inv}|_{dB}}}\, Q_{\mathcal{N}}\left(P_{OUT}\right) \end{aligned} \tag{10}$$

Parameters $\overline{g}^{inv}|_{dB}$, $\sigma^2_{g^{inv}|_{dB}}$ and P_{OUT} are provided to the FBS by the database server. The model for the FBS-to-FMT path gain G_F may also be provided by the database server based on typical values assumed by the operator. Alternatively, they are estimated at each FBS based on MT measurements.

In [5], the FBS power is set according to P_M and I values measured at FBS, assuming that the values of P_M and I are the same for MMTs in Z_{MMT}, except for the wall penetration loss. Equation (10) can be used for setting the FBS power according to FBS power measurements, setting $\sigma_{g^{inv}|_{dB}}$ to a common value, function of the assumed path gain model from MBS to MMT in Z_{MMT}. Thus, $\sigma_{g^{inv}|_{dB}}$ is common to several FBSs, whereas in the proposed location-based approach, $\sigma_{g^{inv}|_{dB}}$ is specific to each FBS. However, as in the location-based approach, $\overline{g}^{inv}|_{dB}$ is specific to each FBS. It is obtained from FBS power measurements $\hat{P}_{M,FBS}$ and $\hat{I}_{FBS}$ of the DL signals from neighbouring MBSs:

$$\overline{g^{inv}}|_{dB} \approx g^{-1}\left(\hat{P}_{M,FBS} + A_w, \hat{I}_{FBS} + A_w, g_{th}\right)|_{dB} \tag{11}$$

Thus, the location-based approach provides more information on actual P_M and I values experienced at MMTs and avoids wall penetration loss error effects on these variables. For situations where the indoor and outdoor received powers from MBS are very different, a better macro-femto performance trade-off can be achieved by the power setting thanks to the additional information provided by the database. Furthermore, an error on penetration loss has more impact on the FBS measurement based power setting approach [5] since A_w appears in (11) in addition to (10), where it impacts $\overline{G}_F|_{dB}$. This performance advantage has some costs: maintaining a database, adding some MBS-to-server signaling in the core network and having a positioning capability in FBSs and many MTs. However, we note that the positioning capability is already well spread among MTs. Furthermore, the database size is relatively small. For instance, for a database density of 0.1 MMT measurement (sample) per m^2, around 10^{11} samples are needed to cover 10^6 km^2. Thus, the database size is of the order of magnitude of one terabyte.

TABLE I: Simulated propagation model for MBS.

Total MBS transmit power	43 dBm
Distance dependent mean path loss (dB)	$128.1 + 37.6\log_{10}(d)$, d in km
MBS antenna type	directional (for 3-sectorized sites) with vertical selectivity
MBS Antenna gain	14 dB
Shadowing standard deviation	8 dB
Shadowing correlation for two MBSs	0.5
Shadowing correlation distance	50 m
Wall penetration loss A_w	10 dB
Small-scale channel	SCM Urban Macro low-spread

TABLE II: Simulated propagation model for FBS.

Maximum FBS transmit power	20 dBm
Distance dependent mean path loss for indoor (dB)	$37 + 30\log_{10}(d)$, d in m
Distance dependent mean path loss for outdoor (dB)	$37 - 6.7\log_{10}(r) + A_w$ $-36.7\log_{10}(d)$, d in m
FBS antenna type	Omni-directional
FBS antenna gain	5 dB
Shadowing standard deviation for FBS	10 dB
Shadowing correlation distance	Uncorrelated
Wall penetration loss A_w	10 dB
Small-scale channel	ITU-InH

IV. Performance results

A. Simulation scenario

We simulate an LTE system with 2 GHz carrier frequency, using a static multi-cell system-level simulator. MBSs are deployed with 1732 m inter-site distance according to the 3GPP case 3 [9]. Nineteen tri-sectorized sites (3 cells per site) are simulated with wrap-around. The indoor femto propagation model is the 3GPP LTE-A femto-cell model and the indoor-to-outdoor femto propagation model uses the attenuation coefficient of the ITU-UMi NLOS model [9]. This approach with double slope more realistically models the difference between indoor-to-indoor and indoor-to-outdoor propagation, which is important for our study. These models include the shadowing on path gain, the Rice factor, the delay spread and the angular spread at base stations and MTs. The small-scale Rayleigh channels follow the 3GPP-SCM-Urban Macro model with low angular spread for MBS and the ITU-InH channel model [9] for FBS. Model details are gathered in Tables I and II.

We consider different deployment scenes, each scene corresponding to one realization of FBS positions and shadowing. For each scene, we consider random drops of MMTs and FMTs. There are 10 MMTs per macro-cell and 2 FMTs per FBS. In each base station, an equal number of sub-carriers is allocated to all MTs and all base stations have full load. Round-Robin scheduling is used, allocating to a MT non-adjacent physical resource blocks (PRBs) of 12 sub-carriers.

TABLE III: Simulated 3GPP-LTE physical layer.

Modulation waveform	OFDM
Bandwidth	10 MHz
FFT size	1024
Useful sub-carriers	600
Sub-carrier spacing	15 kHz
MMT/FMT allocation granularity	one PRB = 12 sub-carriers
Maximum spectral efficiency	7 b/s/Hz (MIMO 2x2, 64-QAM, coderate 1, 43% overhead)

Multi-stream 2x2 multiple-input multiple-output (MIMO) transmission is performed on a 10 MHz system bandwidth as described in Table III. We use a link level to system level interface which takes into account small-scale effects, computing the spectral efficiency with true small-scale interference modeled using a frequency-selective and spatially colored additive Gaussian noise covariance matrix, from large-scale parameters generated by the system level simulation. The spectral efficiency is computed as the outage capacity based on Shannon capacity and is limited here to a maximum 2-stream LTE spectral efficiency, i.e., 7 bits/s/Hz.

Circular FBS buildings with radius $r = 6$ m are assumed. The HIRZ is defined as a ring centered on FBS with 6 m inner radius and 16 m outer radius.

B. Error model used for power and localization measurements

We assume a zero-mean iid Gaussian error model for positioning and for received power measurements $\hat{P}_{M,i}$ and $\hat{I}_i$ in dB. Without any power measurement and positioning errors and with a high database density, the distribution of P_M and I estimated from the database exactly matches the long-term reality. With positioning errors smaller than the shadowing correlation distance, this distribution remains an accurate estimate. We observed from our simulations that for positioning errors higher than the shadowing correlation distance (up to 100 m RMSE), the variance of the distribution becomes over-estimated whereas its mean value remains reliable. Furthermore, practical errors on power estimates (root mean square error (RMSE) smaller than 3 dB) do not strongly impact the performance if there are many MMT measurements available in the database for HIRZ. Indeed, with our scenario, the standard deviation in HIRZ without any power or positioning error is around 4 dB. As the proposed location-based FBS power setting approach is long-term, a high density database is easily built. Thus, in the sequel, we consider 0.1 sample per m^2 for all simulations, i.e., on average 70 MMT measurements in HIRZ.

Furthermore, in the path gain model between FBS and an MMT located in HIRZ, we consider a Gaussian error, iid among FBSs, between the actual wall penetration loss in the FBS building and the assumed wall penetration loss A_w in the algorithm in dB. When not specified, no error is considered.

For comparison, we consider the approach based on the measurement of received powers P_M and I at FBS [5]. FBS measurements suffer from a iid Gaussian error, with a RMSE different from MMT measurements, in order to take into account the positive impact of time averaging and the negative impact of shadowing decorrelation between indoor and outdoor.

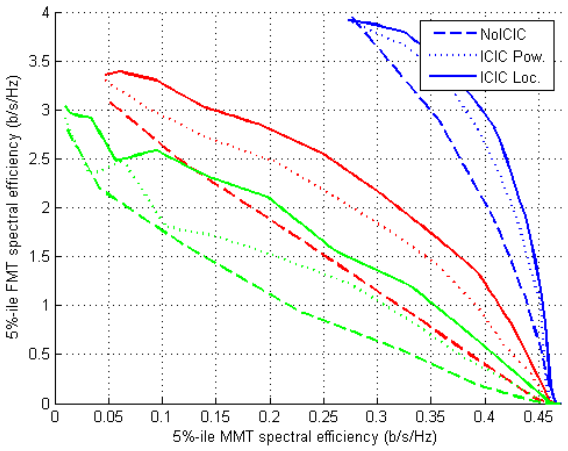

Fig. 2: Global FMT-MMT performance trade-off in term of cell-edge spectral efficiency. Blue: 25 FBS/km^2, red: 125 FBS/km^2, green: 250 FBS/km^2.

C. Simulation results

We simulate 20 realizations of FBS positions and shadowing map for each FBS density and 50 MMT drops for each realization. We compare three approaches: the constant FBS transmit power, the FBS power setting based on FBS power measurement [5] and the proposed location-based FBS power setting (denoted by *NoICIC*, *ICIC Pow.* and *ICIC Loc.*, respectively). In order to compare their effect on FBS and MBS performances, many power setting parameter values and fixed transmit powers are tested.

We evaluate the global FMT-MMT performance trade-off, i.e., the 5%-ile FMT spectral efficiency over all FBSs as a function of the 5%-ile MMT spectral efficiency over all outdoor MMTs. We consider typical measurement errors, namely 10 m RMSE for the location-based approach and 5 dB (resp. 3 dB) RMSE on FBS (resp. MMT) power measurement. Three FBS densities are considered: 25, 125 and 250 FBSs per km^2, i.e., 22, 109 and 217 FBSs per MBS sector, respectively. We observe in Fig. 2 non-negligible femto-femto interference when the FBS density increases since the maximum FBS performance strongly depends on the FBS density. Figure 2 also shows that the proposed location-based power setting exhibits a better FMT-MMT performance trade-off than the two other approaches, the relative gain increasing with the FBS density.

We note that, for FBS, the localization is done once and for all and a good accuracy can be reached even for indoor FBS. For MMT positions, only high quality location information (e.g., with GNSS, using a quality metrics) can be stored in the database. However, an interesting aspect is the sensitivity to localization errors. Figure 3 shows, for the

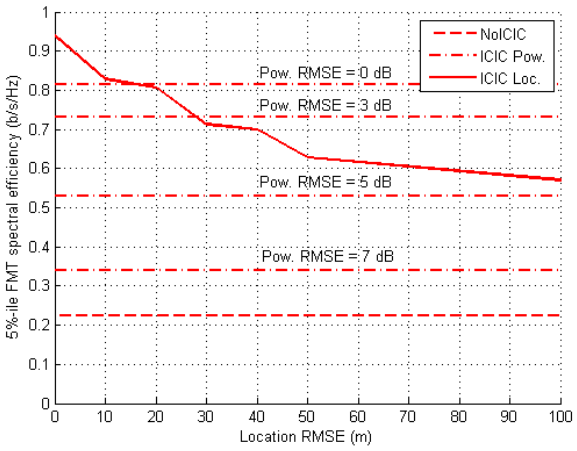

Fig. 3: Localization error effects: Femto performance for 10 % cellular cell-edge decrease with 125 FBS/km^2

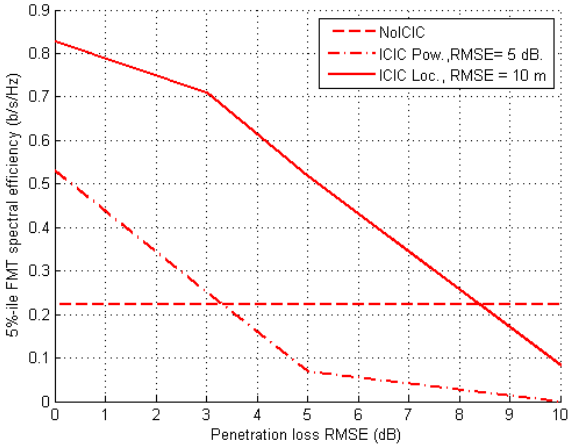

Fig. 4: Penetration loss error effects: Femto performance for 10 % cellular cell-edge decrease with 125 FBS/km^2

three approaches and in medium FBS density, the FMT cell-edge spectral efficiency for a 10 % degradation of MMT cell-edge spectral efficiency (i.e., a 0.42 b/s/Hz spectral efficiency) as a function of positioning RMSE. With typical FBS power measurement RMSE of at least 3 dB, the proposed location-based approach outperforms the simpler FBS power measurement based approach of [5] for positioning RMSE lower than 30 m. For a 20 m RMSE, the FMT cell-edge spectral efficiency is increased by more than 50 % (resp. 10 %) over the FBS power measurement based approach with a 5 dB (resp. 3 dB) RMSE on FBS power measurement. Compared to the constant transmit power approach, it is increased whatever the positioning accuracy (RMSE lower than 100 m) by up to 400 %.

Considering now the sensitivity to wall penetration loss error and assuming typical 10 m, 3 dB and 5 dB RMSE for positioning, MMT power measurements and FBS power measurements, respectively, and medium FBS density, Fig. 4 confirms the lower sensitivity of the proposed location-based approach compared to the FBS power measurement based approach. For 3 dB wall penetration loss RMSE, the power measurement based approach does not outperform the constant FBS transmit power approach whereas the proposed location-based approach still exhibits a 300 % gain over the constant FBS transmit power approach. With 7 dB wall penetration loss RMSE, the location-based approach still outperforms the two other approaches.

V. Conclusion

Long-term power setting for femto-macro ICIC can take benefit from positioning. The concept of HIRZ for controlling the macro degradation due to FBS transmission is used, resulting in an equalization of the macro-degradation among FBSs. The positioning information is used in conjunction with a database available in the core network, providing relevant information to each FBS on powers measured by MMTs in its vicinity. This information guarantees efficient power setting. In the simulated 3GPP-LTE context, the proposed power setting relying on positioning and database improves the global FMT-MMT performance trade-off compared to constant FBS transmit power and the FBS power setting based on FBS power measurement proposed in [5] and proves robustness against relatively high positioning error. Compared to the FBS power setting in [5], higher robustness against wall penetration loss error is also observed.

Acknowledgment

This work has been performed in the framework of the FP7 project ICT-248894 WHERE2 (Wireless Hybrid Enhanced Mobile Radio Estimators - Phase 2) which is partly funded by the European Union.

References

[1] V. Chandrasekhar, J. G. Andrews, and A. Gatherer, "Femtocell networks: A survey," *IEEE Commun. Mag.*, vol. 46, no. 9, pp. 59–67, Sep. 2008.

[2] D. López-Pérez, A. Valcarce, G. de la Roche, and J. Zhang, "OFDMA femtocells: A roadmap on interference avoidance," *IEEE Commun. Mag.*, vol. 47, no. 9, pp. 41–48, Sep. 2009.

[3] V. D'Amico, A. Dekorsys, A. Gouraud, S. Kaiser, B. L. Floch, P. Marsch, and H. Schneich, "ARTIST4G: A way forward to the interference problem in future mobile networks," in *Future Network and Mobile Summit 2010 Conference Proceedings*, Jun. 2010.

[4] G. Fodor, C. Koutsimanis, A. Rácz, N. Reider, A. Simonsson, and W. Muller, "Intercell interference coordination in OFDMA networks and in the 3GPP long-term evolution system," *Journal of Communications*, vol. 4, no. 7, pp. 445–453, Aug. 2009.

[5] J. Guillet, L. Brunel, and N. Gresset, "Downlink femto-macro ICIC with blind long-term power setting," in *Proc. IEEE Personal, Indoor and Mobile Radio Communications, PIMRC*, vol. 22, Toronto, Canada, Sep. 2011, pp. 72–76.

[6] 3GPP, "TDD Home eNode B (HeNB) radio frequency (RF) requirements analysis," 3GPP TSG-RAN - E-UTRA, Tech. Rep. 36.922 V9.0.0, Apr. 2010.

[7] V. Chandrasekhar, M. Kountouris, and J. G. Andrews, "Coverage in multi-antenna two-tier networks," *IEEE Trans. Wireless Commun.*, vol. 8, no. 10, pp. 5314–5327, Oct. 2009.

[8] S. Plass and R. Raulefs, "Combining wireless communications and navigation - the WHERE project," in *Proc. IEEE Vehicular Technology Conference, VTC*, vol. 68, Calgary, Canada, Sep. 2008.

[9] 3GPP, "Further advancements for E-UTRA physical layer aspects," 3GPP TSG-RAN - E-UTRA, Tech. Rep. 36.814, Mar. 2010.